NASA TECHNICAL REPORT

NASA TR R-469

NASA TR R-469

THE EIGENVALUE SPECTRUM OF THE ORR-SOMMERFELD PROBLEM

Basil N. Antar

George C. Marshall Space Flight Center
Marshall Space Flight Center, Ala. 35812

NATIONAL AERONAUTICS AND SPACE ADMINISTRATION • WASHINGTON, D. C. • OCTOBER 1976

1. REPORT NO. NASA TR R-469	2. GOVERNMENT ACCESSION NO.	3. RECIPIENT'S CATALOG NO.
4. TITLE AND SUBTITLE The Eigenvalue Spectrum of the Orr-Sommerfeld Problem		5. REPORT DATE October 1976
		6. PERFORMING ORGANIZATION CODE
7. AUTHOR(S) Basil N. Antar		8. PERFORMING ORGANIZATION REPORT # M-188
9. PERFORMING ORGANIZATION NAME AND ADDRESS George C. Marshall Space Flight Center, Marshall Space Flight Center, Alabama 35812		10. WORK UNIT NO.
		11. CONTRACT OR GRANT NO.
12. SPONSORING AGENCY NAME AND ADDRESS National Aeronautics and Space Administration, Washington, D.C. 20546		13. TYPE OF REPORT & PERIOD COVERED Technical Report
		14. SPONSORING AGENCY CODE

15. SUPPLEMENTARY NOTES

Prepared by Space Sciences Laboratory, Science and Engineering

16. ABSTRACT

A numerical investigation of the temporal eigenvalue spectrum of the Orr-Sommerfeld equation is presented. Two flow profiles are studied, the plane Poiseuille flow profile and the Blasius boundary layer (parallel) flow profile. In both cases a portion of the complex c-plane bounded by $0 \leqslant c_r \leqslant 1$ and $-1 \leqslant c_i \leqslant 0$ is searched and the eigenvalues within it are identified. The spectra for the plane Poiseuille flow at $\alpha = 1.0$ and $R = 10^2, 10^3, 6 \times 10^3$, and 10^4 are determined and compared with existing results where possible. The spectrum for the Blasius boundary layer flow at $\alpha = 0.308$ and $R = 998$ was found to be infinite and discrete. Other spectra for the Blasius boundary layer at various Reynolds numbers seem to confirm this result. The eigenmodes belonging to these spectra were located and discussed.

17. KEY WORDS Hydrodynamic stability; boundary layers; boundary layer transition; eigenvalue problems; numerical methods	18. DISTRIBUTION STATEMENT Unclassified - Unlimited. Cat. 34

19. SECURITY CLASSIF. (of this report)	20. SECURITY CLASSIF. (of this page)	21. NO. OF PAGES	22. PRICE
Unclassified	Unclassified	43	$3.75

* For sale by the National Technical Information Service, Springfield, Virginia 22161

ACKNOWLEDGMENTS

The author wishes to thank Dr. Leslie M. Mack of the Jet Propulsion Laboratory for supplying an unpublished manuscript. Also, special thanks are due to Drs. George H. Fichtl and Frank G. Collins for the many stimulating discussions and helpful suggestions during the course of this investigation. The author also wishes to thank the Associateship Office of the National Academy of Sciences/National Research Council and NASA-George C. Marshall Space Flight Center for their support.

TABLE OF CONTENTS

LIST OF ILLUSTRATIONS

LIST OF TABLES

THE EIGENVALUE SPECTRUM OF THE ORR-SOMMERFELD PROBLEM

I. INTRODUCTION

This report is primarily concerned with a numerical investigation of the temporal eigenvalue spectrum of the Orr-Sommerfeld equation. The solution and the general properties of this equation are still a topic of interest nearly seven decades after its formulation. The long-standing interest in the problem is primarily due to two reasons. The first reason is due to physical considerations in that the equation has served as a successful model for the study of the linear stability of one class of hydrodynamic flows, namely, that of parallel flows. The second, and more abstract, reason is due to the complex mathematical structure of the equation, whereby this equation, together with the one-dimensional Schroedinger equation, belongs to a class of linear differential equations that contain a large parameter and turning points. This equation is further complicated by the fact that it is a non-self-adjoint problem. The derivation of the Orr-Sommerfeld equation for the linear stability problem together with an excellent discussion of its solution can be found in the classical monograph by Lin [1]. A comprehensive historical survey on the solution and the properties of a whole class of differential equations to which this problem belongs is discussed by McHugh [2].

In this report only one property of this problem which has received attention recently will be studied, namely, the type of the eigenvalue spectrum of the equation. The knowledge of whether this equation possesses an infinite or a finite spectrum is necessary for one method of study of the nonlinear hydrodynamic stability problem because, as shown by Eckhaus [3], the solution of the nonlinear problem may be obtained through an expansion in terms of the eigenfunctions of the linear problem. Hence, it is necessary to show that the linear problem possesses a complete set of eigenfunctions. Also, there is the more fundamental issue which requires the proof that the eigenfunctions of the linear problem form a complete set. This is necessary to determine the class of initial disturbances that may be investigated by the method of normal modes.

In principal, the completeness property has been neglected in the past for many reasons, and one of them may have been that a completeness proof for the general non-self-adjoint problems simply does not exist in the mathematical literature. However, the first to brave that hurdle was Schensted [4], who proved an expansion theorem for the Orr-Sommerfeld equation for two specific flow profiles, namely, the plane Poiseuille flow and the pipe flow. This effort was followed sometime later by DiPrima and Habetler [5] who proved a completeness theorem for the general linear stability problem for bounded flow profiles. However, to date there is no proof of a similar theorem for the stability problem of the boundary layer flow because this flow profile is semi-infinite; i.e., the flow is bounded by a wall on one side and extends to infinity on the other. Also, the controversy surrounding the nature of the eigenvalue spectrum of the Orr-Sommerfeld equation for the boundary layer flow has not been settled yet.

Of course, the only way to settle this issue is by a rigorous mathematical proof similar to the one given by Schensted for the bounded flow situation. However, it is possible to explore this question, in principle at least, through an investigation similar to the one presented herein. Indeed, two such attempts have been undertaken recently, one by Jordinson [6] and the other by Mack [7]. In these studies it was shown through a search in a finite portion of the eigenvalue plane that there exist only a few eigenvalues of the equation, leading to the conjecture that the eigenvalue spectrum for the boundary layer profile is finite. However, the number and location of these eigenvalues varied from one search to the other. In this report it will be shown that the eigenvalue spectrum of the Orr-Sommerfeld equation for the boundary layer profile may be infinite. Also, this investigation will show that the findings of both Jordinson and Mack are not contradictory within the framework of these respective studies.

Because of the complexity of the equation, closed form analytical solutions are precluded in this study and the problem will be investigated through numerical approximations only. There are many numerical techniques in the literature for solving the Orr-Sommerfeld eigenvalue problem, but none is suited for the present investigation. Most of these methods fall within two general classes, the matrix method and the shooting method. In the former, the differential eigenvalue problem is reduced to an algebraic problem through various approximations to the solution. The most widely used of these methods is the finite difference approximation technique such as the one used by Jordinson [8]. Another example of this class is the Chebyshev Polynomial Approximation method such as the one employed by Benek [9]. However, these methods possess two shortcomings that preclude their use in the present investigation. One is that the number of eigenvalues sought and determined is directly proportional to the number of mesh points used or the number of terms retained in the polynomial approximation. The second deficiency is that these methods do not provide for an a priori control on the section of the complex eigenvalue plane that needs to be searched.

As for the shooting method, the boundary value problem is solved as a system of initial value problems by choosing a suitable guess on the missing initial conditions. The equations are then numerically integrated to the desired end point, where the guessed initial conditions are corrected through the requirement that the equations satisfy the given end condition. For this purpose, an iterative procedure such as the Newton-Raphson-Kantorovich method may be used. In linear problems such as this one, only one iteration is necessary to determine the missing initial conditions and eigenvalues. This method has been extensively used by many investigators, such as Mack [10] and Davey [11]. However, the technique possesses a major shortcoming in the sense that only one eigenvalue may be determined at a time, and in order to start the iterative process and have the iterations converge, it is necessary to have a good estimate of the eigenvalues that need to be determined. This is obvious since most iterative processes are local in nature. Previously, such good estimates on the eigenvalues were determined from the known approximate analytical solutions or by a variational method such as that of Lee and Reynolds [12]. However, when such estimates do not exist or are cumbersome to produce, the method will involve trial and error procedures that may be very costly and frustrating.

It is clear from the literature survey that the known numerical techniques are not adequately suited for the present investigation and that a new method must be developed to carry out the desired study satisfactorily. Such a method is developed here. It belongs to the shooting method class and has the additional advantage that it is capable of locating more than one eigenvalue at a time and does not require an initial guess. The method is global in the sense that all the eigenvalues that lie within a finite region of the eigenvalue plane are identified and determined. The method is also automatic in the sense that once the boundaries of the domain desired to be searched are given, it proceeds to locate the eigenvalues without any further information from the operator. Also, the technique has the built-in capability of determining multiplicities of the eigenvalues if any exist.

II. THEORETICAL BACKGROUND

In this section the theoretical background that is necessary for the development of the numerical technique for the present investigation is outlined for the general linear differential eigenvalue problem. However, before entering into this discussion, the specific problem that will be studied later will be defined so that it may serve as a guide in the development of the technique.

The specific equation that will be studied is the one governing the amplitude function of a two-dimensional, wave-like, infinitesimal perturbation in an otherwise stationary, two-dimensional flow, namely,

$$(D^2 - \alpha^2)^2 \, \phi = i \, \alpha \, R \, [(u - c)(D^2 - \alpha^2)\, \phi - \phi \, D^2 u] \quad , \tag{1}$$

where D denotes differentiation with respect to the spatial coordinate y. Equation (1) is commonly known as the Orr-Sommerfeld equation in which ϕ is the complex amplitude function; α and c are the disturbance wave number and speed, respectively, while u(y) is the stationary velocity profile that is assumed to be defined throughout the range of integration. R is the Reynolds number which is defined by UL/ν, where ν is the kinematic viscosity. All of the variables in equation (1) have been made dimensionless with respect to a suitable length scale L and a velocity scale U.

The appropriate boundary conditions for equation (1) which are physically viable are either the no-slip conditions at a solid boundary or the requirement that the perturbation decay to zero at infinity when the fluid is infinite in extent. Such boundary conditions are commonly known as homogeneous,' and the specific conditions for the cases that will be studied will be specified separately later. Equation (1) and the homogeneous boundary conditions form an eigenvalue problem, and it is our task herein to investigate the nature of the eigenvalue spectrum which belongs to this problem.

Equation (1) may be written in a general operator form,

$$L_1 \phi + c L_2 \phi = 0 \quad , \tag{2}$$

where

$$L_1 \equiv (D^2 - \alpha^2)^2 - i \alpha R [u(D^2 - \alpha^2) - D^2 u] \tag{3a}$$

$$L_2 \equiv i \alpha R (D^2 - \alpha^2) \quad , \tag{3b}$$

where the wave speed $c = c_r + ic_i$ is taken to be the eigenvalue. However, any other combination of the parameters that appear in equation (1) may be taken as eigenvalues.

Let us consider a general differential eigenvalue problem of the form (2); i.e.,

$$L_1 \phi + \lambda L_2 \phi = 0 \quad , \tag{4}$$

where L_1 and L_2 are linear differential operators of the form,

$$L(\phi) = p_0(y) D^n \phi + p_1(y) D^{n-1} \phi + \cdots + p_n(y) \phi \quad . \tag{5}$$

For the cases of interest here, we need to limit outselves for the case where the order of L_2 is less than or equal the order of L_1. λ in equation (4) is the complex eigenvalue, and ϕ is the complex eigenfunction of the real variable y. Let us assume that the coefficients of equation (5), $p_k(y)$, possess continuous derivatives up to order n on the interval of integration [a,b]. Also let the differential equation (4) be subject to the following homogeneous boundary conditions:

$$B_i(\phi) = 0 \quad (i = 1, \cdots, n) \quad , \tag{6}$$

which are specified at both ends of the interval [a,b]. Note that the boundary conditions $B_i(\phi)$ may be composed of linear combinations of the 2n quantities,

$$\begin{aligned} &\phi(a),\ D\phi(a),\ \cdots,\ D^{n-1}\phi(a) \\ &\phi(b),\ D\phi(b),\ \cdots,\ D^{n-1}\phi(b) \end{aligned} \tag{7}$$

Let us now define the determinant $f(\lambda)$ by

$$f(\lambda) = \det \begin{bmatrix} B_1(\phi_1) & \cdots & B_1(\phi_n) \\ \vdots & & \vdots \\ B_n(\phi_1) & \cdots & B_n(\phi_n) \end{bmatrix} \tag{8}$$

where $\phi_1, \phi_2, \ldots, \phi_n$ is a fundamental system of Cauchy solutions of equation (4) collectively satisfying linearly independent sets of initial conditions at $y = a$. If the coefficients of the differential operators L_1 and L_2, namely, $p_k(y)$, and the boundary conditions $B_i(\phi)$ are independent of the eigenvalue λ, the following theorem concerning the eigenvalues of equation (4) may be invoked, Naimark [13]: *The eigenvalues of the operators of equation (4) together with the boundary conditions of (6) are the zeroes of the function $f(\lambda)$. If $f(\lambda)$ vanishes identically, then any number λ is an eigenvalue of the problem defined by (4) and (6). If, however, $f(\lambda)$ is not identically zero, equation (4) has at most denumerably many eigenvalues and the eigenvalues have no finite limit point.*

It can also be shown [13] that when the differential operators L_1 and L_2 are not singular, then $f(\lambda)$ is an integral analytic function of λ. This last property is of primary importance for the development of our numerical scheme, as will be shown.

Thus, at least in principle, the problem of locating the eigenvalues of equation (4) together with the boundary conditions given by (6) is determined. However, determining the zeroes of the function $f(\lambda)$ is more complicated, and the common procedure in the past has been to determine only one zero at a time. This was accomplished, as explained in Section I, through local iterative techniques that require a good initial guess to begin them. However, if one is able to generate a global technique for determining the zeroes of $f(\lambda)$, one possesses the capability of determining more than one, or all, of the eigenvalues of the problem defined by (4) and (6) at one time. Toward this end one may use the following theorem from the theory of complex analysis which provides the means for locating all of the zeroes of a complex function in a finite region of the complex plane. This theorem may be stated in the following way: *If γ is a regular curve in a simply connected open set not passing through any zero or pole of a meromorphic function $f(\lambda)$ in that set, the integral*

$$\frac{1}{2\pi i} \int_{\gamma} \frac{f'(\lambda)}{f(\lambda)} \, d\lambda \tag{9}$$

is equal to the excess of the number of zeros over the number of poles of $f(\lambda)$ inside γ (a pole or zero of order k counting as k poles or zeros, respectively).

Since, as mentioned earlier, $f(\lambda)$ in our specific problem is an analytic function of λ, then within any closed region in the λ-plane there does not exist any pole; hence, expression (9) may be modified to read

$$\frac{1}{2\pi i} \int_{\gamma} \frac{f'(\lambda)}{f(\lambda)} \, d\lambda = N \quad , \tag{10}$$

where N is the number of zeros within the curve γ. Furthermore, the above theorem admits a simple generalization that may be valuable later. Again, let $f(\lambda)$ be analytic inside and on γ and let $\omega(\lambda)$ be also analytic inside and on γ. Then we have the following result:

$$\frac{1}{2\pi i} \int_{\gamma} \omega(\lambda) \frac{f'(\lambda)}{f(\lambda)} \, d\lambda = \sum_{r=1}^{N} q_r \, \omega(\lambda_r) \quad , \tag{11}$$

where the sum is taken over the zeros of $f(\lambda)$, and q_r is the order of the zeros λ_r. The proof of expression (11) may be found in Goodstein [14].

To carry out our investigation, the previous two theorems together with expression (11) will be used in the form of numerical approximations. The details of such approximations will be discussed in Section III.

III. NUMERICAL DETAILS

A. The Numerical Evaluation of the Zeros of a Complex Function

As outlined in Section II, the procedure for locating the eigenvalues of the differential eigenvalue problem reduces to locating the zeros of the complex function f(c) provided that f(c) could be determined at an arbitrary number of points (hereinafter c will replace λ used previously). The procedure for the numerical evaluation of f(c) and f′(c) for any value of c will be discussed later. Note that because of the complexity of equation (1), f(c) can only be evaluated numerically; however, for a less complex equation it might be possible to evaluate this function in a closed form and thus alleviate the necessity for a numerical investigation. Assuming temporarily that f(c) and f′(c) may be evaluated around any contour γ, then the zeros of that function may be located through the use of expressions (10) and (11) in the following manner (a detailed discussion on the technique that is outlined here may be found in Reference 15).

First, the number of zeros inside a prescribed region of the complex c-plane, here this region is taken to be a circle, may be determined numerically through an appropriate quadrature formula approximation for expression (10). Once the number of zeros inside γ, N for example, is determined, their location may be found in the second step. By letting the function $\omega(\lambda)$ in (11) take successively the values $c, c^2, c^3, \ldots, c^N$, all the power sums of the zeros inside γ may be determined by performing the following N contour integrations:

$$s_1 = \int_\gamma c \frac{f'(c)}{f(c)} dc = \sum_{j=1}^{N} c_j$$

$$s_2 = \int_\gamma c^2 \frac{f'(c)}{f(c)} dc = \sum_{j=1}^{N} c_j^2 \tag{12}$$

$$s_N = \int_\gamma c^N \frac{f'(c)}{f(c)} dc = \sum_{j=1}^{N} c_j^N \quad ,$$

where c_j denotes all the zeros of f(c) inside γ. Again, the numerical values of the contour integrals in (12) may be obtained through an appropriate quadrature formula.

Using the complex numbers $s_1 s_2, \ldots, s_N$, a polynomial P(c) of degree N may be constructed whose zeros inside γ coincide with the zeros of f(c). Note that this polynomial is not an approximation of the function f(c). For the construction of such a polynomial, Newton's formula is used in which the coefficients of the polynomial P(c) are evaluated from the power sums of the roots of the polynomial. Once the equivalent polynomial, P(c), is constructed, any polynomial root finder may be employed to extract the zeros of P(c). The zeros of f(c) are coincident with the roots of P(c) inside γ. The specific polynomial root finder subroutine used in the present investigation utilizes the quadratic method. It should be mentioned that the numerical technique for finding the zeros of the function f(c) as described previously is also capable of determining multiplicities of the zeros if any exist. However, multiple zeros were not found in the present problem within the domain of search.

As for the numerical evaluations of the quadrature integrals in (10) and (12), the following formula developed by Delves and Lyness [15] for the integration around a circle in the complex plane was employed. Let the contour of integration, γ, be the circle $\gamma(c_0, r)$ whose center is c_0 and radius is r; upon translating the center of the circle to the origin, these quadrature expressions may be written as integrals with respect to the parameter t in the following way:

$$\frac{s_N}{r^N} = \int_0^1 \exp\,[2\pi i(N+1)t]\; r\, \frac{f'\,[c_0 + r\exp(2\pi i t)]}{f[c_0 + r\exp(2\pi i t)]}\, dt \quad , \tag{13}$$

where N, which is the number of zeros inside γ, is set equal to zero when evaluating the quadrature integral of (10). Upon using the trapezoidal rule for approximating the quadrature integral in (13), we obtain the following numerical formula for the integration around the circle

$$\frac{s_N}{r^N} = \frac{1}{m} \sum_{j=1}^{m} \psi_N\,(j/m) \;+\; 0\,(A^m) \quad . \tag{14}$$

ψ_N is the integrand in (13), and m is the number of discrete points around the circle γ at which $f'(c)/f(c)$ is evaluated. A in (14) is defined by

$$A = \max\,(A_1, A_2) \quad , \tag{15}$$

where

$$|A| < 1$$

$$A_1 = \max_{r_j < r} r_j/r$$

$$A_2 = \max_{r_j > r} r/r_j$$

where r_j is the distance between the center and the closest zero to the perimeter of the circle γ. Formula (14) is convenient in that by increasing the number of function evaluations around the perimeter of γ from m to 2m requires only m additional function evaluations. Also, it is notable that the convergence of (14) to (13) is linear; i.e., for each additional function evaluation the error is reduced by a constant factor.

B. The Numerical Evaluation of f′(c)

An examination of the quadrature expressions (10) and (11) reveals that the evaluation of the derivative of f(c) with respect to c is necessary for the implementation of the root finding procedure. This derivative may be obtained by the usual rule of determinant differentiation that requires the evaluation of the derivative of each element of (8) with respect to c. To achieve this, the differential system (2) is augmented with yet another system of the same order governed by the following differential equation:

$$L_1 \Phi + c L_2 \Phi + L_2 \phi = 0 \quad , \tag{16}$$

where $\Phi = \partial\phi/\partial c$. The differential operators L_1 and L_2 in equation (16) are the same as those defined by (3). Note that since f is an analytic function of c, the differentiation may be taken with respect to either c_r or c_i without any loss of generality. Equation (16) is then solved subject to the following initial conditions:

$$\Phi(a) = D\Phi(a) = 0 = D^2\Phi(a) = D^3\Phi(a) \quad . \tag{17}$$

C. The Initial Value Integrators

It is obvious from the previous discussion that to determine the eigenvalues to equation (1) inside the contour γ, the functions f(c) and f′(c) need to be determined numerically at discrete points along the perimeter of the circle γ. These values may be obtained by evaluating the determinant in expression (8) for f(c) and a similar *determinant for f′(c), where each column of the determinant represents* a Cauchy solution of equation (1). Naturally, each Cauchy solution involves an initial value integration of equation (1) over the interval [a,b] with the appropriate initial condition.

The forward integrators used in the present study are of the Runge-Kutta-Nyström type for a system of second-order ordinary differential equations. This integrator utilizes the fact that the differential operators L_1 and L_2 do not possess any odd order derivatives, leading to a reduction of the computation time of the whole system by approximately one-half over the classical Runge-Kutta methods for first-order equations. While many extensive higher order formulas with step size control exist [16], the specific integrator used here is a seventh-order Runge-Kutta-Nyström with a fixed step size.

The Orr-Sommerfeld equation (1) presents difficulty when it is numerically integrated as an initial value problem because some of the parameters that appear in the equation are widely separated. This is apparent when it is observed that the wave number α is of order 10^{-1} while the Reynolds number for any problem of interest is of order 10^3 or more. Since in the numerical integration of this equation one begins with a system of linearly independent (orthogonal) initial vectors, because of the wide separation of the parameters, these vectors become increasingly parallel as the integration proceeds to the final point, resulting in their being linearly dependent and rendering the matrix for the determinant (8) ill-conditioned.

Few methods have been devised to overcome this situation, and, to the author's knowledge, they are all implementations of one basic idea. Since the initial vectors were orthogonal, it is necessary to ensure that the solution vectors remain orthogonal throughout the range of integration. This is achieved by reorthonormalizing the solution vectors at discrete points along the path of integration. Such a technique was first developed by Godunov [17], which was later improved by Conte [18], whereby the Gramm-Schmidt orthonormalization technique is employed. In the present study, however, because equation (16) is also being integrated simultaneously with (1), one must ensure that the solution vectors of (16) are transformed in the same manner as those of (1). That is, if the solution vectors of (1), for example $\bar{\phi}_1$ $\bar{\phi}_2, \ldots, \bar{\phi}_n$, are transformed to $\bar{\psi}_1, \bar{\psi}_2, \ldots, \bar{\psi}_n$ through the transformation

$$\begin{bmatrix} \bar{\psi}_1 \\ \bar{\psi}_2 \\ \vdots \\ \bar{\psi}_n \end{bmatrix} = [P] \begin{bmatrix} \bar{\phi}_1 \\ \bar{\phi}_2 \\ \vdots \\ \bar{\phi}_n \end{bmatrix} , \qquad (18)$$

at some point along the integration interval the solution vector of (16), for example $\bar{\Phi}_1, \bar{\Phi}_2, \ldots, \bar{\Phi}_n$, should be transformed at that point by

$$\begin{bmatrix} \bar{\Psi}_1 \\ \bar{\Psi}_2 \\ \vdots \\ \bar{\Psi}_n \end{bmatrix} = [P] \begin{bmatrix} \bar{\Phi}_1 \\ \bar{\Phi}_2 \\ \vdots \\ \bar{\Phi}_n \end{bmatrix} \tag{19}$$

where [P] is the orthonormalization transformation matrix at the point in question.

IV. THE PLANE POISEUILLE FLOW

A. Definition of the Problem

This type of profile is distinguished by the fact that the flow is bounded between two parallel stationary planes located at $y = \pm 1$. The stationary laminar profile for this configuration is a parabolic function of y given by

$$u(y) = 1 - y^2 \quad . \tag{20}$$

The length scale L for this problem is half the channel width, while the velocity scale U is the maximum velocity midway between the planes. The boundary conditions appropriate to equation (1) for this case are the usual no-slip conditions at the walls, which may be written as

$$\phi(\pm 1) = 0 = D\phi(\pm 1) \quad . \tag{21}$$

Since the mean flow profile in expression (20) and the boundary condition are symmetric in y, then the solution for equation (1) may be split into odd and even parts. Thus, for solving the present eigenvalue problem it is sufficient to consider either the odd or even solutions. Splitting the problem in this manner permits the solution of equation (1) for the half-range [0, 1] in place of the full range [-1, 1] by replacing the condition at one wall with the following conditions at the center of the channel:

$$D\phi(0) = D^3\phi(0) \qquad \text{for the even solution} \qquad (22a)$$

and

$$\phi(0) = D^2\phi(0) \qquad \text{for the odd solution} \quad , \qquad (22b)$$

thus permitting the reduction of the integration interval by one-half. Although the present technique of eigenvalue search applies equally well for either the even or the odd solution, only the even solution will be investigated here.

With the problem and boundary conditions thus defined, the determinant in expression (8) will then take the following form:

$$f(c) = \det \begin{bmatrix} D\phi_1(0) & D\phi_2(0) & D\phi_3(0) & D\phi_4(0) \\ D^3\phi_1(0) & D^3\phi_2(0) & D^3\phi_3(0) & D^3\phi_4(0) \\ \phi_1(1) & \phi_2(1) & \phi_3(1) & \phi_4(1) \\ D\phi_1(1) & D\phi_2(1) & D\phi_3(1) & D\phi_4(1) \end{bmatrix} \quad . \qquad (23)$$

This determinant is of high order requiring the solution of four Cauchy problems and may be reduced considerably in the following manner. Since the boundary conditions (21) and (22) are separable with two of them applying at $y = 1$ and the remaining two at $y = 0$, a reduction of the order of the determinant may be achieved by solving an initial value problem defined by augmenting the given conditions at $y = 0$ by two further sets of two linearly independent conditions at that point. When the resulting fundamental solutions are $\bar{\phi}_1$ and $\bar{\phi}_2$, where $\bar{\phi}_i = (\phi_i, D\phi_i, D^2\phi_i, D^3\phi_i)$, expression (23) may then be replaced by the characteristic determinant equation expressing the compatibility of a nontrivial combination of these solutions and their derivatives with the given boundary conditions at $y = 1$; namely,

$$f(c) = \det \begin{bmatrix} \phi_1(1) & \phi_2(1) \\ D\phi_1(1) & D\phi_2(1) \end{bmatrix} \quad . \qquad (24)$$

Thus, the solution of two rather than four Cauchy problems is sufficient, resulting in a great labor savings. The linearly independent initial vectors for these two Cauchy problems are:

$$\bar{\phi}_1(0) = (1, 0, 0, 0)$$

$$\bar{\phi}_2(0) = (0, 0, 1, 0) \tag{25}$$

Thus, the forward integration is started at $y = 0$, with (25) as initial conditions; f(c) is then determined by evaluating the determinant given by (24) at $y = 1$. A similar procedure is followed for the determination of f′(c).

B. The Search Technique

The following search procedure in the eigenvalue plane was employed in this investigation. The region desired to be searched was spanned by circles of uniform radius as shown in Figure 1 in such a way as to cover the entire desired search area by a minimum number of circles. Although it is desirable to span the complete domain of interest by one circle, it was found that there exists an upper limit on the size of the individual search contour. It was observed that whenever the radius of the circle in question was greater than a certain value, the quadrature formula as given by (14) failed to converge. The value of the maximum radius allowable was found to be dependent on the Reynolds number in equation (1); i.e., the smaller the Reynolds number was, the larger was the allowable value of the radius.

Thus, using the technique outlined previously, each circle was then searched for eigenvalues within it. To begin the individual search, f(c) and f′(c) were evaluated initially at eight equally spaced points around the circumference of the circle. The number of points was then doubled, and the quadrature value obtained from the 8- and the 16-point approximations of (14) were compared. When the difference in the value of s_i between the two iterations was less than 1 percent, the quadrature value was considered converged. If, however, this criterion was not met, the number of function evaluations around the perimeter was doubled and the convergence criteria were tested again.

All of the computations reported hereafter were performed on the IBM 360/65 computer in double precision arithmetic when possible. Since the time required for each function evaluation is considerable (for each such evaluation, the integration of 16 real second-order differential equations over the interval [0,1] was necessary), the computation time for the search of each circle is directly proportional to the final number of function evaluations around the perimeter. For example, the time required for 128 such evaluations was approximately 3 minutes of computation time. More details on computation times and accuracies may be found elsewhere [19].

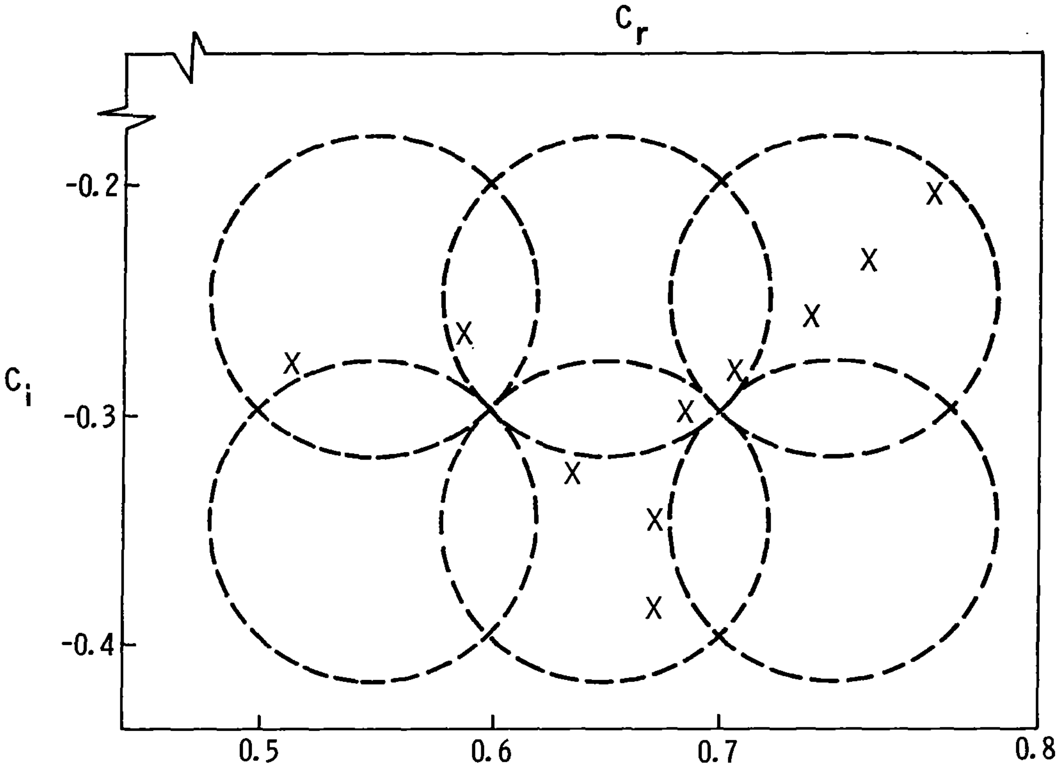

Figure 1. A portion of the complex c-plane indicating the method of search for eigenvalues within a specified region of that plane (X indicates eigenvalues found inside the specific circles).

C. Results

As discussed in Section I, the eigenvalue spectrum of the Orr-Sommerfeld equation for the plane Poiseuille flow has been investigated in earlier works, but none of these investigations dealt in depth with an eigenvalue search. The only complete search to date is that of Mack. Employing a different search scheme from the present one, Mack has tabulated the 32 known symmetric eigenmodes for $\alpha = 1.0$ and $R = 10\,000$ that lie within the rectangle $0 \leqslant c_r \leqslant 1.0$ and $-1.0 \leqslant c_i \leqslant 0$ in the complex c-plane. Hence, the results of the present scheme for that particular case will be compared with Mack's tabulation.

All of the eigenvalues that were found in the region $0 \leqslant c_r \leqslant 1.0$ and $-1.0 \leqslant c_i \leqslant 0$ for the parameters $\alpha = 1.0$ and $R = 10\,000$ are tabulated in Table 1 and plotted in Figure 2. These eigenvalues agree as to location and number with those of Mack, and no

TABLE 1. EIGENVALUES FOR THE PLANE POISEUILLE FLOW AT $\alpha = 1.0$ AND $R = 10\,000$ IN THE REGION OF THE c-PLANE BOUNDED BY $0.0 \leqslant c_r \leqslant 1.0$ AND $-1.0 \leqslant c_i \leqslant 0.0$.

A Family		P Family		S Family	
c_r	c_i	c_r	c_i	c_r	c_i
0.2381	+0.0038	0.9636	−0.0362	0.6776	−0.3437
0.3487	−0.1245	0.9383	−0.0614	0.6745	−0.3898
0.1894	−0.1828	0.9071	−0.0922	0.6673	−0.4316
0.4749	−0.2087	0.8798	−0.1194	0.6723	−0.4833
0.3685	−0.2388	0.8515	−0.1474	0.6716	−0.5324
0.5871	−0.2672	0.8231	−0.1755	0.6710	−0.5833
0.5129	−0.2866	0.7948	−0.2035	0.6704	−0.6359
0.6829	−0.3076	0.7665	−0.2316	0.6700	−0.6903
0.6361	−0.3252	0.7381	−0.2597	0.6720	−0.7436
		0.7089	−0.2877	0.6692	−0.8044
				0.6689	−0.8642
				0.6687	−0.9258
				0.6685	−0.9893

different eigenvalues were found in this region. Following the nomenclature adopted by Mack, these modes may be classified into three distinct families; the A, P, and S families. This classification is somewhat natural because of the peculiar shape of the eigenvalue spectrum. Two parts of the spectrum extend along approximately straight lines; these are labeled the P and S families. The remaining part of the spectrum does not conform to such a pattern and will comprise the A family.

It is the members of the S family that are of interest in the speculation of whether the spectrum is finite or infinite. The eigenmodes of this family lie along a vertical line at the approximate location of $c_r = 0.667$ and extend to as large a value of $-c_i$ as one cares to pursue. Thus, the members of this family are inferred to be infinite in extent, which is in agreement with the theoretical conclusion that the spectrum of this problem is infinite and discrete.

From the practical point of view, it is the members of the A family that are of interest because it was found that at least one eigenvalue of this family is always the least stable. This is apparent when one compares the spectra for various Reynolds numbers and a fixed α.

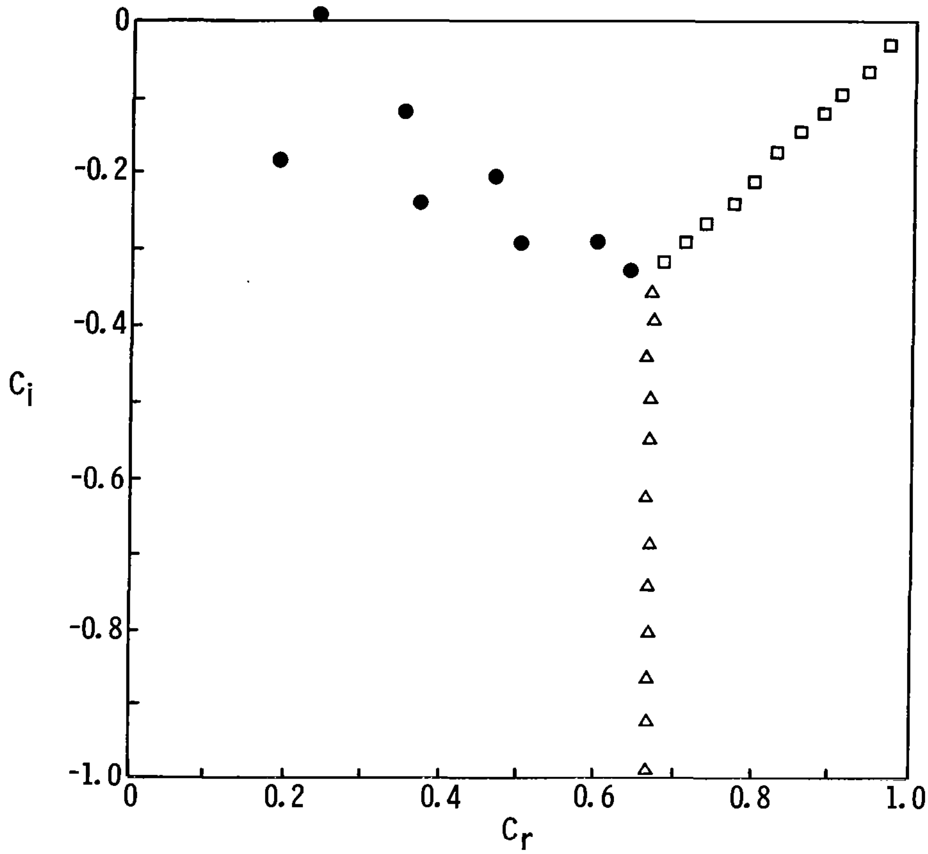

Figure 2. All of the eigenvalues found within the indicated boundaries in the c-plane for the plane Poiseuille flow at $\alpha = 1.0$ and R = 10 000 (● indicates members of the A family; □ indicates members of the P family; and Δ indicates members of the S family).

To form a general picture of the behavior of the eigenvalue spectra at various values of R and a fixed α, the eigenvalue spectra for $\alpha = 1$ and $R = 10^2$, 10^3, and 6×10^3 are presented in Figures 3 through 5 for comparison. Also, these eigenvalues are tabulated in Table 2. It is obvious from comparing these spectra that the density of eigenvalues in all the families increases with the increase in Reynolds numbers. However, the general character of the spectrum is invariant with Reynolds number. Also, in all of these spectra the infinite character of the S family is preserved.

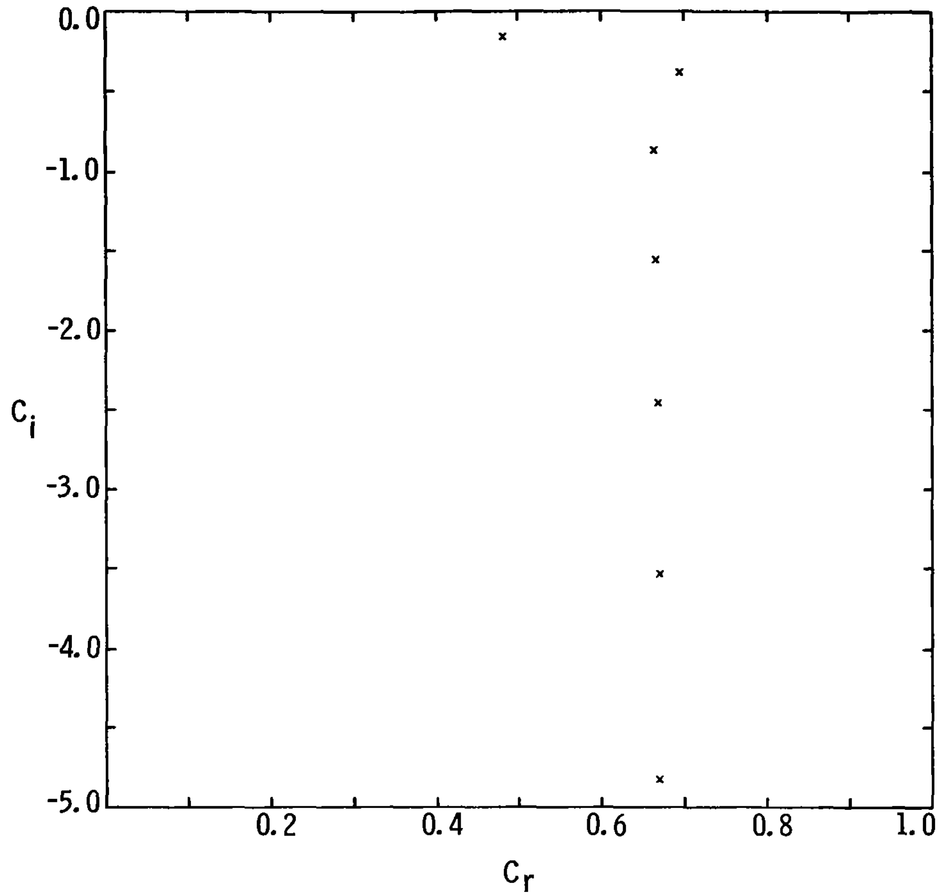

Figure 3. All of the eigenvalues found within the indicated boundaries in the c-plane for the plane Poiseuille flow at $\alpha = 1.0$ and $R = 100$.

V. THE BLASIUS BOUNDARY LAYER FLOW

A. Definition of the Problem

Although the differential equation investigated for the Blasius boundary layer flow is the same as for the plane Poiseuille flow (differing only in the character of the coefficients of the equation), these two problems are completely distinct from the mathematical point of view. The differences are in the boundary conditions that need to be satisfied. In the plane Poiseuille flow the boundaries are at finite distances, while in the Blasius boundary layer flow one boundary extends to infinity. This last feature distinguishes most external flows from internal flows which are characterized by finite boundaries.

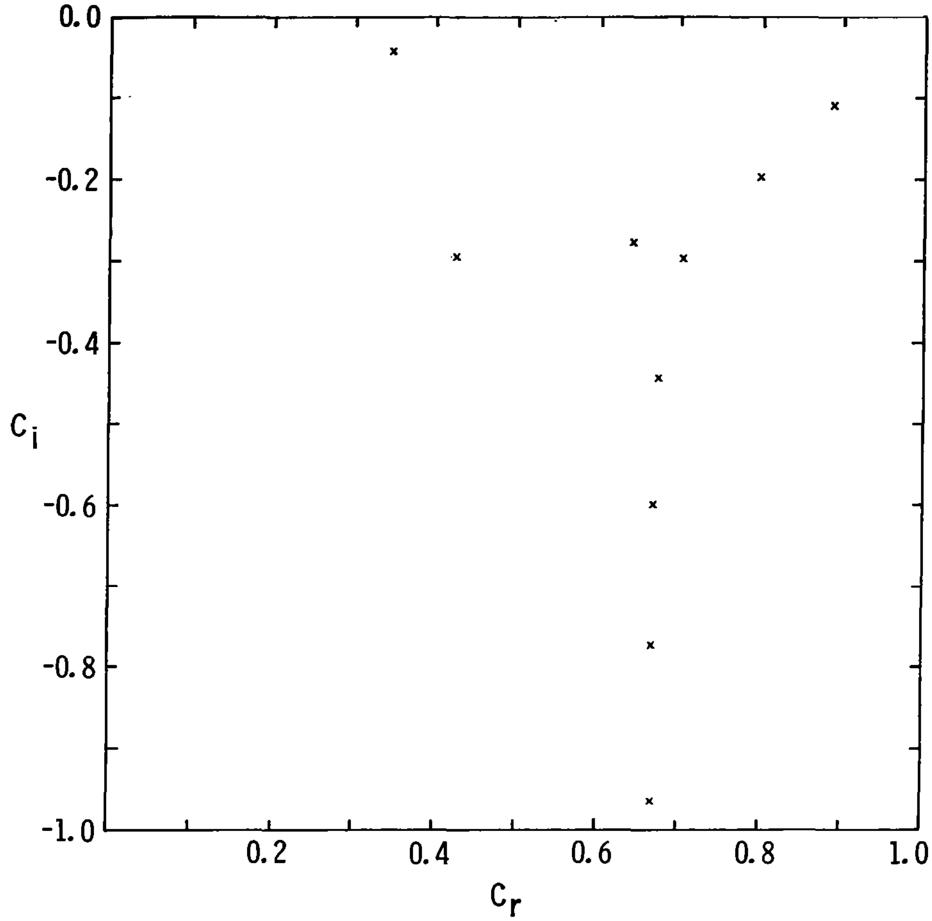

Figure 4. All of the eigenvalues found within the indicated boundaries in the c-plane for the plane Poiseuille flow at $\alpha = 1.0$ and $R = 1000$.

Another difference in the two flows that needs to be emphasized concerns the parallel flow assumption that was used to derive equation (1). While this assumption is appropriate for the plane Poiseuille flow and a host of other physically realizable flows, it is not a strictly valid assumption for the boundary layer flow. However, results derived from equation (1) under this assumption for the boundary layer flow have been used in the past as a close approximation to the real problem. It is with this reservation that we approach the analysis for the Blasius boundary layer profile.

In the past many results have been built on the premise that equation (1) possesses an infinite set of eigenfunctions with their respective eigenvalues for the Blasius boundary layer flow. Hence, it is considered both instructive and worthwhile to show

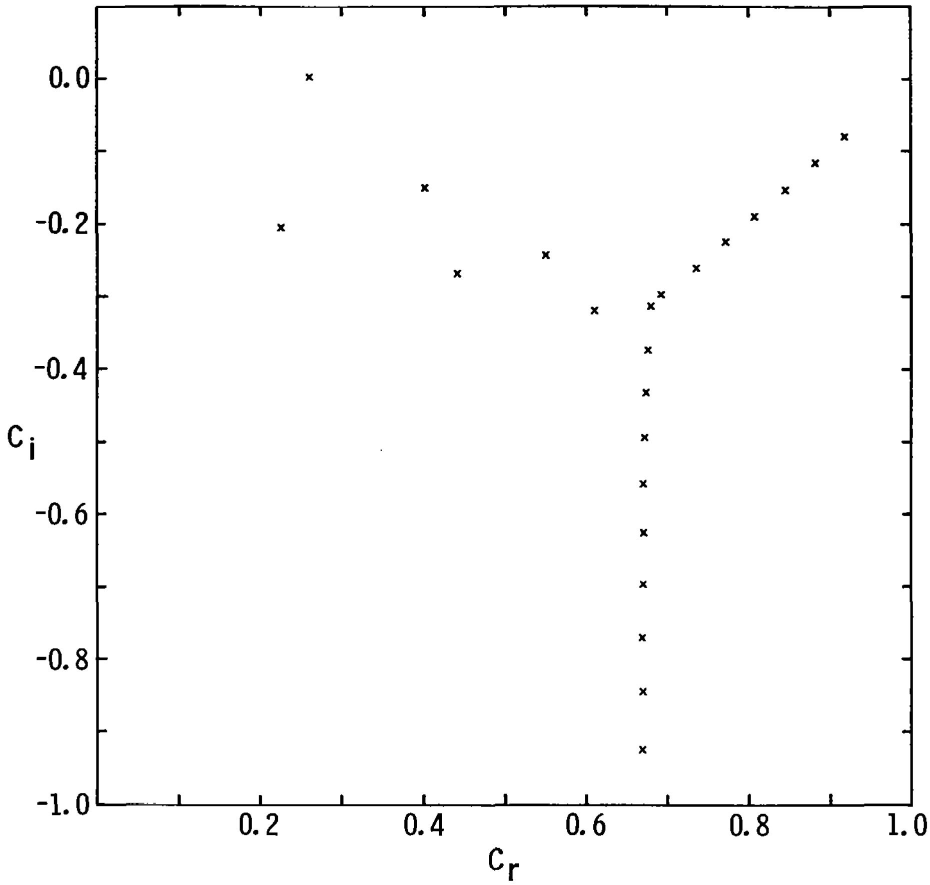

Figure 5. All of the eigenvalues found within the indicated boundaries in the c-plane for the plane Poiseuille flow at $\alpha = 1.0$ and R = 6000.

whether such a spectrum exists. As far as the present analysis is concerned, the distinguishing feature of the problem lies in the fact that the flow is only bounded at one wall and is free at the other end. A flow of this type is commonly known as semi-infinite. The mean velocity profile for the Blasius boundary layer flow is given by

$$u(y) = F'(y) \quad , \tag{26}$$

where F(y) is the stream function that is given by the well-known Blasius equation

$$F'''(y) + K^2 F(y) F''(y) = 0 \tag{27}$$

TABLE 2. EIGENVALUES FOR THE PLANE POISEUILLE FLOW AT $\alpha = 1.0$ AND VARIOUS R VALUES IN THE REGION OF THE c-PLANE BOUNDED BY $0.0 \leqslant c_r \leqslant 1.0$ AND $-5.0 \leqslant c_i \leqslant 0.0$ FOR R = 100, AND $0.0 \leqslant c_r \leqslant 1.0$ AND $-1.0 \leqslant c_i \leqslant 0$ FOR R = 1000 AND 6000.

$\alpha = 1.0$					
R = 100		R = 1000		R = 6000	
c_r	c_i	c_r	c_i	c_r	c_i
0.47849	−0.16295	0.34628	−0.04213	0.25980	+0.00032
0.69316	−0.38258	0.42700	−0.29538	0.91782	−0.08151
0.66166	−0.87322	0.64309	−0.27822	0.88128	−0.11765
0.66351	−1.56515	0.70554	−0.29722	0.40027	−0.15257
0.66491	−2.45548	0.67397	−0.44457	0.84473	−0.15378
0.66556	−3.54274	0.79849	−0.19757	0.80817	−0.18991
0.66589	−4.82693	0.88813	−0.11008	0.22543	−0.20621
		0.66924	−0.59967	0.77159	−0.22605
		0.66805	−0.77344	0.54890	−0.24377
		0.66755	−0.96552	0.73482	−0.26242
				0.43985	−0.26845
				0.89266	−0.29762
				0.67834	−0.31461
				0.60960	−0.32006
				0.67598	−0.37438
				0.67322	−0.43342
				0.67199	−0.49486
				0.67110	−0.55915
				0.67039	−0.62632
				0.66980	−0.69643
				0.66933	−0.76953
				0.66893	−0.84566
				0.66860	−0.92484

Equation (27) has been made dimensionless here in such a manner as to let it have the same independent variable, y, as the one in the perturbation equation (1). The parameter K in equation (27) relates the well-known Blasius similarity variable η to y by $\eta = Ky$, where $K = \lim_{\eta \to \infty} [\eta - F(\eta)]$. The reference length for this case is the boundary layer displacement thickness δ_1, and the reference velocity is the free stream velocity. Hence the Reynolds number is the one based on the boundary layer displacement thickness.

The boundary conditions appropriate for this problem are the usual no-slip, no-penetration conditions at the wall given by

$$\phi(0) = 0 = D\phi(0) \tag{28}$$

together with the requirement that the perturbation function be bounded for large values of y; i.e.,

$$\phi(\infty) \ , \ D\phi(\infty) \to 0 \quad \text{as} \quad y \to \infty \quad . \tag{29}$$

Upon inspecting conditions (28) and (29), it appears that it is desirable to evaluate the secular determinant (8) in terms of the wall conditions only. Here an argument for the reduction of the order of the determinant from four to two may be followed in a manner analogous to the one presented for the plane Poiseuille flow problem of Section IV. To evaluate the secular determinant at the wall, the forward integration of the two Cauchy problems is begun at the free stream end, where the asymptotic properties of equation (1) are exploited and carried on to the wall end where conditions (28) are valid. The free stream initial conditions may be generated by observing that equation (1) is extremely simplified for large y; namely, as $y \to \infty$, $u(y) \to 1$ and $D^2 u(y) \to 0$, leading to a constant coefficient equation whose solution may be written explicitly in terms of the following four exponential functions:

$$\phi_{1,2}(y_1) = \exp(\pm \alpha y_1)$$

$$\phi_{3,4}(y_1) = \exp(\pm p y_1) \quad , \tag{30}$$

where

$$p = [\alpha^2 + i \alpha R (1 - c)]^{1/2} \quad , \quad \text{Real}(p) \geqslant 0 \quad .$$

In (30) y_1 is some arbitrarily chosen large value of y that will be discussed further in the next subsection. Now, condition (29) may be used to eliminate the two solutions with the positive exponential sign in (30). Thus, the two Cauchy problems may be integrated from the free stream starting with the following two linearly independent initial vectors:

$$\bar{\phi}_1(y_1) = (1, -\alpha, \alpha^2, -\alpha^3) \exp(-\alpha y_1)$$

$$\bar{\phi}_2(y_1) = (1, -p, p^2, -p^3) \exp(-p y_1) \tag{31}$$

Then, the secular determinant that needs to be evaluated at the wall, $y = 0$, will be given by

$$f(c) = \begin{bmatrix} \phi_1(0) & \phi_2(0) \\ D\phi_1(0) & D\phi_2(0) \end{bmatrix} \tag{32}$$

B. Results

As discussed in Section I, there does not exist any mathematical proof on the nature of the eigenvalue spectrum for this problem; however, there are two numerical investigations on the character of this spectrum. One by Jordinson [6], which is considered of a somewhat limited extent, and another more thorough investigation by Mack. Since both of these investigations were carried out for the parameters $\alpha = 0.308$ and $R = 998$, these parameters will be used initially for the search procedure to facilitate comparison.

The rectangle in the complex c-plane bounded by $0 \leqslant c_r \leqslant 1.0$ and $-1.0 \leqslant c_i \leqslant 0$ was searched for eigenvalues with the parameters $\alpha = 0.308$ and $R = 998$. Again, as was done for the plane Poiseuille flow, the rectangle was spanned by a number of small overlapping circles in such a way as to cover all the desired search area. All of the eigenvalues found in this rectangle for this case are shown in Figure 6 and are tabulated in Table 3. The value of y_1 for the initial conditions (31) which was employed in this search was 6.0. This represents a length of approximately 1.5 times the boundary layer thickness and thus was deemed suitable.

The structure of the eigenvalue spectrum as shown in Figure 6 is similar to the spectra of the plane Poiseuille flow that was discussed earlier. Hence, the classification of the spectrum into the A, P, and S families is appropriate for this case also. Note that the

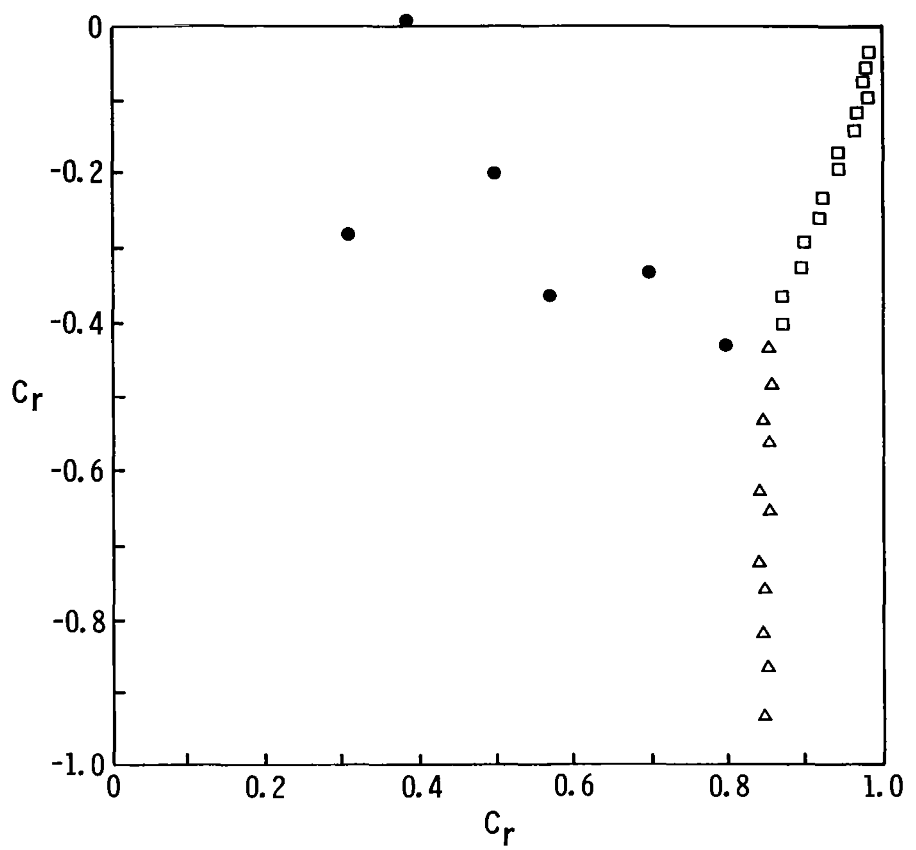

Figure 6. All of the eigenvalues found within the indicated boundaries in the c-plane for the Blasius boundary layer flow at $\alpha = 0.308$, R = 998, and $y_1 = 6.0$ (● indicates members of the A family; □ indicates members of the P family; and Δ indicates members of the S family).

spectrum had only one mode possessing $c_i > 0$, which is the commonly known unstable mode. Again, the P and S families occupied regions in the c-plane similar to their counterparts for the plane Poiseuille flow with the exception that they did not fall strictly on two straight lines. The members of these families seem to lie along two neighboring lines that are very close to each other. Hence, the members of the S family did not reach a single asymptotic value in c_r, rather the two values of $c_r \approx 0.85$ and $c_r \approx 0.84$. However, the modes of this family did extend to as large a value of $-c_i$ as was carried out in the search procedure.

TABLE 3. EIGENVALUES FOR THE BLASIUS BOUNDARY LAYER AT $\alpha = 0.308$, $R = 998$, AND $y_1 = 6.0$ IN THE REGION OF THE c-PLANE BOUNDED BY $0.0 \leqslant c_r \leqslant 1.0$ AND $-1.0 \leqslant c_i \leqslant 0.0$.

A Family		P Family		S Family	
c_r	c_i	c_r	c_i	c_r	c_i
0.3642	+0.0079	0.9913	-0.0248	0.8483	-0.4406
0.4839	-0.1921	0.9893	-0.0441	0.8546	-0.4852
0.2897	-0.2769	0.9808	-0.0656	0.8459	-0.5357
0.6863	-0.3308	0.9826	-0.0871	0.8515	-0.5764
0.5572	-0.3654	0.9666	-0.1118	0.8430	-0.6372
0.7939	-0.4342	0.9650	-0.1392	0.8526	-0.6754
--------	--------	0.9501	-0.1661	0.8404	-0.7363
0.8874	-0.4148	0.9474	-0.1955		
		0.9282	-0.2275	0.8491	-0.7823
		0.9229	-0.2625	0.8403	-0.8474
		0.8990	-0.2978	0.8483	-0.8934
		0.8949	-0.3329	0.8298	-0.9611
		0.8726	-0.3670		
		0.8644	-0.4037		

Thus from the character of the members of the S family it may also be concluded that the eigenvalue spectrum of the Orr-Sommerfeld equation for the Blasius boundary layer, as posed in expressions (26), (31) and (32) for the numerical integration, possesses an infinite and discrete number of eigenvalues. However, it was found that the spectrum as shown in Figure 6, and for the parameters used, is not unique. The spectrum depended in a strong manner, as far as location and number of eigenvalues found, on the value of y_1 chosen in the initial conditions (31). However, this common character of the spectrum did not affect the overall character, shape, or the conclusion on the infinity of eigenmodes of the spectrum. To illustrate this dependence of the eigenvalue spectrum on y_1, the spectra at $y_1 = 8.0$, 10.0, and 12.0 are presented in Figures 7 through 9 with the parameter α and R held fixed. Table 4 lists all of the eigenvalues that are shown in Figures 7 through 9 for $c_i > -0.7$.

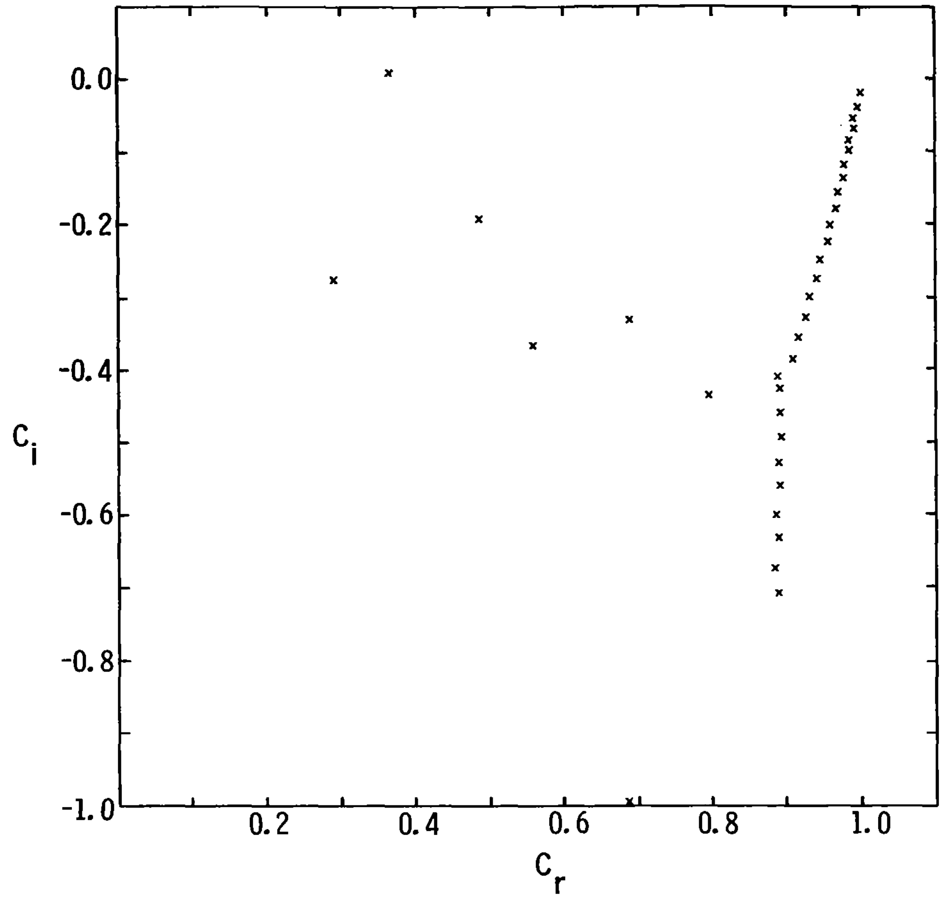

Figure 7. All of the eigenvalues found within $0.0 \leqslant c_r \leqslant 1.0$ and $-0.7 \leqslant c_i \leqslant 0.0$ for the Blasius boundary layer flow at $\alpha = 0.308$, $R = 998$, and $y_1 = 8.0$.

As y_1 was increased to values greater than 6.0, the number and location of the members of the P and S families seemed to vary, while the number and location of the members of the A family remained fixed. With the increase of y_1, the spacings between the modes of the P and S families decreased, resulting in the appearance of new members belonging to these families. Furthermore, the juncture point between the P and S families shifted to higher values of c_r with the increase of y_1. This behavior is clearly portrayed in Figures 6 through 9 and Tables 3 and 4. These figures also illustrate vividly the shift to higher values in c_r of the vertical lines along which the modes of the S family are located with the increase in y_1. It is also clear from these figures that as y_1 is increased, the distance between the adjacent curves, along which the members of the P and S families are located, decreased.

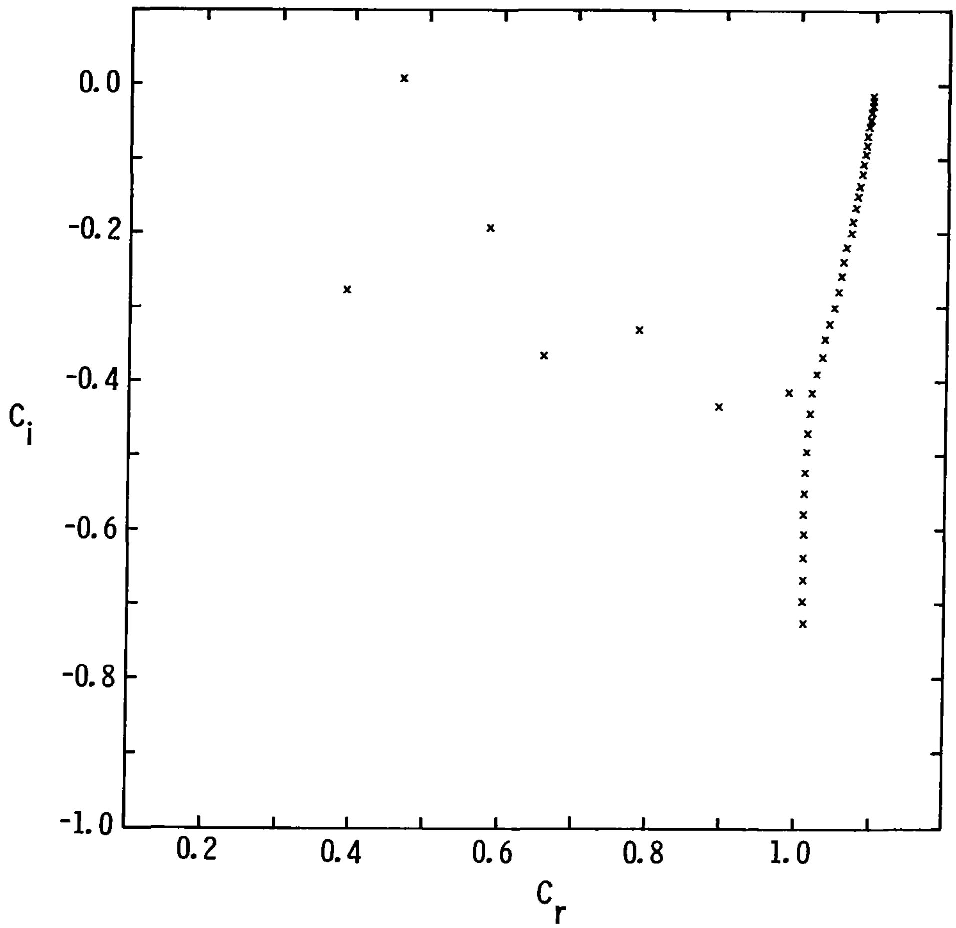

Figure 8. All of the eigenvalues found within $0.0 \leqslant c_r \leqslant 1.0$ and $-0.7 \leqslant c_i \leqslant -0.015$ for the Blasius boundary layer flow at $\alpha = 0.308$, R = 998, and $y_1 = 10.0$.

As the modes of the S family shifted to values in c_r greater than 0.89, an eigenvalue at the location (0.887 – 0.415 i) first appeared. This mode remained in the same position for subsequent shifts to the right of the members of the S family. Since the position of this mode remained fixed with the increase in y_1, it was concluded that it belongs to the A family (in our nomenclature the members of the A family are invariant with y_1) and is listed in Table 3 below the dashed line to identify the way it was located. Such a result then shows that the lines along which the P and S family lie mask any eigenvalue belonging to the A family that lies to the right of these lines; and in order to obtain all the members of the A family, the search must be conducted for a very large value of y_1 such that the P and S family lines have shifted to the rightmost location in the c-plane.

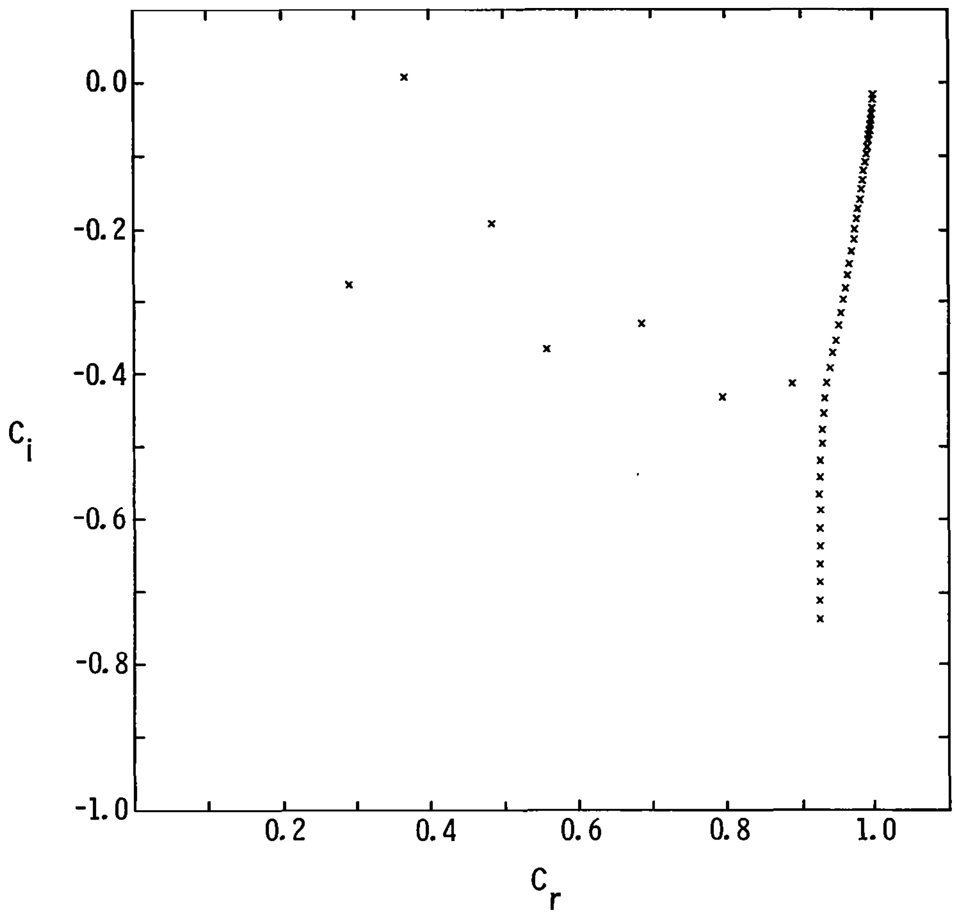

Figure 9. All of the eigenvalues found within $0.0 \leqslant c_r \leqslant 1.0$ and $-0.7 \leqslant c_i \leqslant -0.02$ for the Blasius boundary layer flow at $\alpha = 0.308$, R = 998, and $y_1 = 12$.

A comparison of the spectra shown in Figures 6 through 9 with those obtained by Jordinson and Mack clearly shows that in both of these investigations only parts of the total spectrum were located. By comparing Figure 6 with Figure 1 of Jordinson, it appears that he was able to locate some of the modes of the A and P families. However, there seems to be no indication that he located any modes belonging to the S family. Mack, on the other hand, determined all of the modes of the A family but was not able to locate any mode belonging to the P or S families.

TABLE 4. EIGENVALUES OF THE P AND S FAMILIES FOR THE BLASIUS BOUNDARY LAYER FLOW AT $\alpha = 0.308$, $R = 998$, AND $y_1 = 8.0$, 10.0, AND 12.0 IN THE REGION OF THE c-PLANE BOUNDED BY $0.0 \leqslant c_r \leqslant 1.0$ AND $-0.7 \leqslant c_i \leqslant 0.015$.

$y_1 = 8.0$		$y_1 = 10.0$		$y_1 = 12.0$	
c_r	c_i	c_r	c_i	c_r	c_i
1.00031	-0.01845	0.99822	-0.01645	0.998503	-0.01846
0.99508	-0.03932	0.99830	-0.02194	0.99873	-0.02427
0.98990	-0.05394	0.99798	-0.02979	0.99754	-0.03693
0.99128	-0.06720	0.99603	-0.03780	0.99529	-0.04407
0.98393	-0.08331	0.99404	-0.04833	0.99556	-0.05194
0.98470	-0.09925	0.99322	-0.05679	0.99441	-0.06071
0.97726	-0.11720	0.99106	-0.06837	0.99359	-0.06935
0.97623	-0.13683	0.99086	-0.08032	0.99149	-0.07907
0.96817	-0.15636	0.98707	-0.09244	0.99102	-0.08889
0.96599	-0.17851	0.98715	-0.10625	0.98903	-0.09973
0.95730	-0.20001	0.98261	-0.12046	0.98818	-0.11060
0.95503	-0.22358	0.98127	-0.13572	0.98562	-0.12225
0.94519	-0.24745	0.97666	-0.15078	0.98500	-0.13420
0.94091	-0.27372	0.97544	-0.16706	0.98208	-0.14687
0.93061	-0.29885	0.97064	-0.18387	0.98109	-0.15973
0.92536	-0.32719	0.96891	-0.20154	0.97836	-0.17349
0.91467	-0.35402	0.96357	-0.21970	0.97652	-0.18769
0.90667	-0.38412	0.96096	-0.23902	0.97334	-0.20206
0.88688[a]	-0.40966[a]	0.95572	-0.25789	0.97178	-0.21713
0.89088	-0.42565	0.95271	-0.27897	0.96882	-0.23182
0.89058	-0.45890	0.94642	-0.29858	0.96657	-0.24888
0.89157	-0.49188	0.94341	-0.32155	0.96288	-0.26455
0.88711	-0.52771	0.93603	-0.34213	0.96033	-0.28165
0.88932	-0.55986	0.93373	-0.36601	0.95651	-0.29879
0.88507	-0.59833	0.92495	-0.39026	0.95402	-0.31669
0.88838	-0.63201	0.88736[a]	-0.41476[a]	0.95065	-0.33398
0.88364	-0.67208	0.92047	-0.41521	0.94673	-0.35375
0.88714	-0.70798	0.91635	-0.44367	0.94255	-0.37232
		0.91409	-0.47035	0.93912	-0.39250
		0.91332	-0.49612	0.93521	-0.41315

TABLE 4. (Concluded)

y_1 = 8.0		y_1 = 10.0		y_1 = 12.0	
c_r	c_i	c_r	c_i	c_r	c_i
		0.91084	-0.52386	(0.88743	-0.41472)
		0.91176	-0.54997	0.93224	-0.43476
		0.90944	-0.57897	0.93019	-0.45606
		0.91087	-0.60619	0.92848	-0.47804
		0.90861	-0.63646	0.92790	-0.49909
		0.91011	-0.66501	0.92671	-0.52162
		0.90810	-0.69627	0.92669	-0.54359
		0.90934	-0.72633	0.92547	-0.56691
				0.92584	-0.58977
				0.92466	-0.61395
				0.92521	-0.63772
				0.92406	-0.66279
				0.92474	-0.68741
				0.92359	-0.71338
				0.92436	-0.73887

a. These eigenvalues belong to the A family.

To study the influence of Reynolds number on the character of the eigenvalue spectrum, a second case was investigated in which α was held constant at 0.308 while R was increased to 1720. With this variation the qualitative features of the eigenvalue spectrum did not change from the previous case; i.e., the spectrum again possessed the A, P, and S families. Again, the members of the A family remained invariant with respect to y_1, but now the family was comprised of 9 eigenvalues instead of the 7 of the previous case. Similarly, the variation of the spectrum with y_1 followed the same pattern as the previous case, as shown in the composite graph of Figure 10. In this figure the eigenvalue spectrum for $\alpha = 0.308$ and R = 1720 is shown for y_1 = 7.0, 9.0, and 11.0. Note the shift of the P and S families to the right with the increase in y_1. Also note the invariance of the location of the members of the A family with respect to y_1. Again, the most unstable mode belongs to the A family and it is the commonly known unstable mode. The eigenvalues that are shown in Figure 10 are listed in Tables 5 and 6.

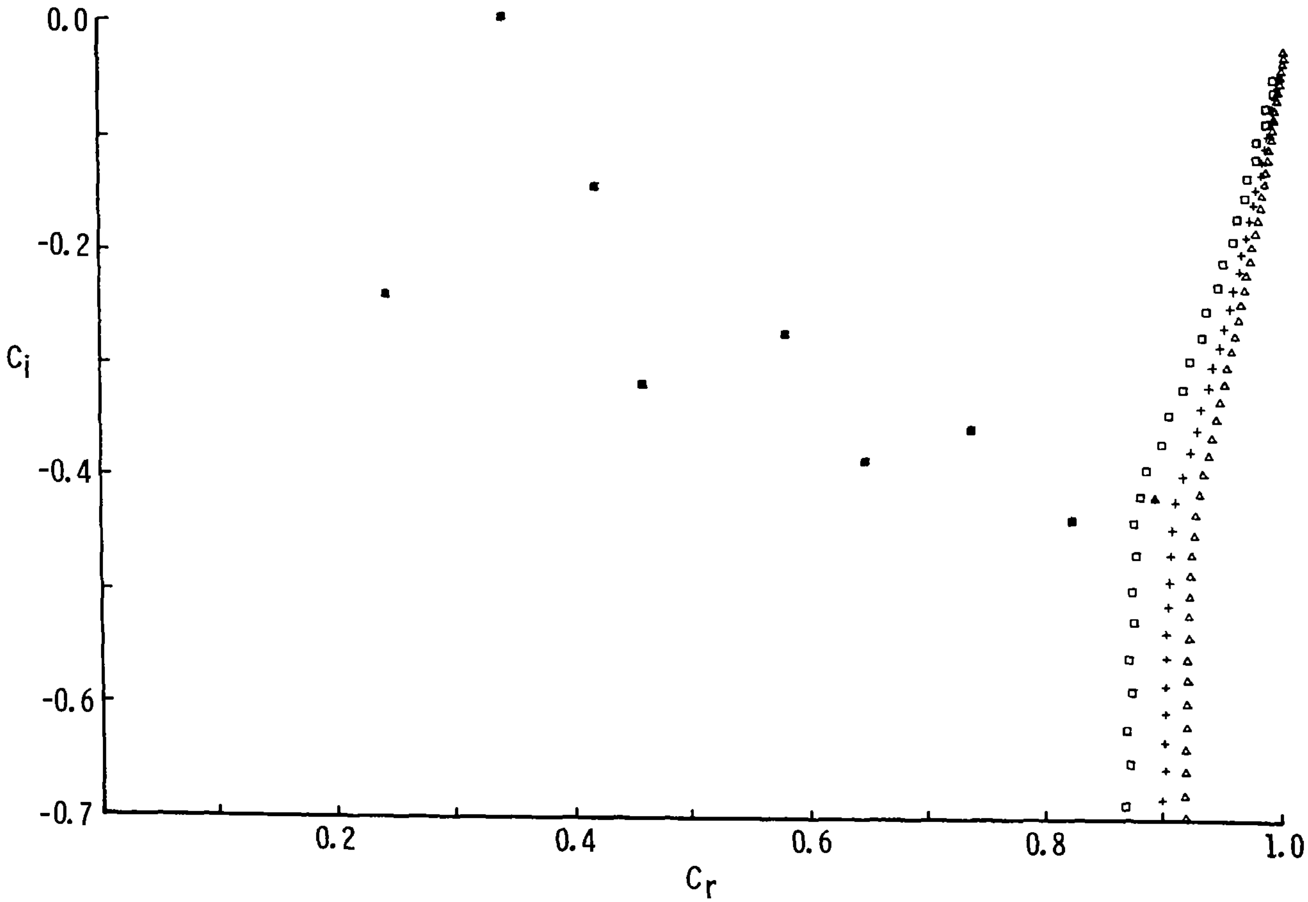

Figure 10. All of the eigenvalues found within $0.0 \leqslant c_r \leqslant 1.0$ and $-0.7 \leqslant c_i \leqslant -0.02$ for the Blasius boundary layer flow at $\alpha = 0.308$ and $R = 1720$ (□ indicates $y_1 = 7.0$; + indicates $y_1 = 9.0$; and Δ indicates $y_1 = 11.0$).

TABLE 5. EIGENVALUES OF THE A FAMILY FOR THE BLASIUS BOUNDARY LAYER FLOW AT $\alpha = 0.308$ AND $R = 1720$ WITHIN THE REGION OF THE c-PLANE BOUNDED BY $0.0 \leqslant c_r \leqslant 1.0$ AND $-1.0 \leqslant c_i \leqslant 0.0$.

c_r	c_i
0.3360	0.0041
0.2412	-0.2390
0.4150	-0.1425
0.4562	-0.3187
0.5775	-0.2730
0.6444	-0.3845
0.7343	-0.3571
0.8189	-0.4348
0.8891	-0.4151

VI. CONCLUSIONS

In this report, a purely numerical scheme was presented for locating the temporal eigenvalues of the Orr-Sommerfeld equation. The method was especially developed for the present investigation to furnish without any ambiguity the information necessary on the location of all of the eigenvalues that lie within the investigated region in the complex c-plane. The technique was then applied in Sections IV and V to perform the desired numerical investigation on the eigenvalue spectrum of the Orr-Sommerfeld equation. First the eigenvalue spectra for the plane Poiseuille flow profile were identified in Section IV for various values of the Reynolds number while keeping the wave number fixed. The search, as expected, did not yield any new information on the nature of the eigenvalue spectra for this flow profile. However, the fact that all of the eigenvalues that were identified in the search did belong to the spectra and no eigenvalue was found that did not belong to it is of greater importance. Hence, it was concluded that the numerics of the method had no appreciable influence on the number and location of these eigenvalues. Furthermore, extensive tests were conducted to study the effects of the numerics on these eigenvalues as they pertain to the integrator step-size, the number of orthonormalizations, and the type of the initial value integrator used. The conclusion was that all of the eigenvalues that were identified with this technique do belong to these spectra.

Once it was confirmed that the method did yield the correct eigenvalues of the problem, the eigenvalue spectrum for the boundary layer profile was investigated in Section V. It is concluded from this study that the spectrum obtained from the

TABLE 6. EIGENVALUES OF THE P AND S FAMILIES FOR THE BLASIUS BOUNDARY LAYER FLOW AT $\alpha = 0.308$, R = 1720, AND y_1 = 7.0, 9.0, AND 11.0 IN THE REGION OF THE C-PLANE BOUNDED BY $0.0 \leqslant c_r \leqslant 1.0$ AND $-0.7 \leqslant c_i \leqslant -0.02$.

$y_f = 7.0$		$y_1 = 9.0$		$y_1 = 11.00$	
c_r	c_i	c_r	c_i	c_r	c_i
0.99758	-0.01031	0.99919	-0.00766		
0.98937	-0.04736	0.99877	-0.01247	0.99764	-0.02277
0.99056	-0.05905	0.99699	-0.02390	0.99784	-0.02725
0.98380	-0.07207	0.99668	-0.02998	0.99662	-0.03287
0.98380	-0.08568	0.99473	-0.03789	0.99658	-0.03873
0.97604	-0.10176	0.99442	-0.04448	0.99487	-0.04495
0.97593	-0.11651	0.99176	-0.05447	0.99502	-0.05128
0.96734	-0.13360	0.99158	-0.06336	0.99337	-0.05850
0.96665	-0.15086	0.98887	-0.07241	0.00308	-0.06573
0.95864	-0.17006	0.98838	-0.08275	0.99053	-0.07366
0.95524	-0.18942	0.98438	-0.09451	0.99068	-0.08164
0.94664	-0.20869	0.98397	-0.10576	0.98875	-0.09040
0.94293	-0.23009	0.97953	-0.11810	0.98814	-0.09910
0.93305	-0.25114	0.97910	-0.13018	0.98583	-0.10840
0.92919	-0.27398	0.97471	-0.14325	0.98528	-0.11783
0.91889	-0.29543	0.97378	-0.15676	0.98223	-0.12785
0.91371	-0.32048	0.96902	-0.17082	0.98206	-0.13796
0.90240	-0.34320	0.96744	-0.18540	0.97926	-0.14871
0.89595	-0.36885	0.96255	-0.20030	0.97831	-0.15981
0.88319	-0.39172	0.96046	-0.21597	0.97563	-0.17088
0.97794[a]	-0.41420[a]	0.95540	-0.23188	0.97439	-0.18257
0.81941[a]	-0.43530[a]	0.95280	-0.24831	0.97135	-0.19453
0.87193	-0.43761	0.94761	-0.26491	0.97009	-0.20686
0.87450	-0.46604	0.94453	-0.28253	0.96681	-0.21930
0.87013	-0.49752	0.93843	-0.30012	0.96538	-0.23222
0.87249	-0.52512	0.93518	-0.31846	0.96201	-0.24556

TABLE 6. (Concluded)

y_1 = 7.0		y_1 = 9.0		y_1 = 11.0	
c_r	c_i	c_r	c_i	c_r	c_i
0.86803	-0.55806	0.92886	-0.33681	0.96011	-0.25889
0.87118	-0.58609	0.92515	-0.35657	0.95682	-0.27301
0.86649	-0.62089	0.91957	-0.37475	0.95439	-0.28720
0.87018	-0.64987	0.91344	-0.39687	0.95073	-0.30155
0.86590	-0.68629	0.88914[a]	-0.41507[a]	0.94838	-0.31631
		0.90667	-0.41935	0.94454	-0.33133
		0.90415	-0.44353	0.94187	-0.34698
		0.90337	-0.46570	0.93801	-0.36246
		0.90100	-0.48885	0.93505	-0.37878
		0.90107	-0.51036	0.93100	-0.39516
		0.89930	-0.53422	0.92782	-0.41256
		0.90069	-0.55630	0.88898[a]	-0.41527[a]
		0.89828	-0.58139	0.92486	-0.43022
		0.89951	-0.60446		
		0.89764	-0.63028	0.92275	-0.44833
		0.89908	-0.65406	0.92185	-0.46570
		0.89661	-0.68109	0.92012	-0.48407
				0.92006	-0.50163
				0.91856	-0.52051
				0.91901	-0.53855
				0.91780	-0.55806
				0.91840	-0.57669
				0.91724	-0.59681
				0.91768	-0.61623
				0.91660	-0.63685
				0.91730	-0.65677
				0.91620	-0.67817
				0.91689	-0.69866

a. These eigenvalues belong to the A family.

numerical solution of the problem, as was posed, is infinite and discrete. It should be remembered, however, that this conclusion is only valid for the numerically approximated problem and is not valid for the originally posed problem which is somewhat different. This is so because in the process of the numerical approximation to the solution, the Orr-Sommerfeld equation was discretised over the finite interval $[0, y_1]$, where at the point y_1 the original boundary conditions were replaced with a matched approximated analytical solution. Thus due to the restructuring of the problem in the process of the numerical solution, the original semi-infinite problem $[0, \infty)$ is in effect transformed to a finite interval problem.

This conclusion on the eigenvalue spectrum for the boundary layer profile does seem, at first, in contradiction with the conclusion reached by Mack, i.e., that the spectrum consisted only of the modes of the A family. But upon a closer examination of Mack's results and taking into account the findings of Jordinson (6) and Benek (9), it may be concluded that the eigenvalue spectrum for this problem is as given in Figures 6 through 10. It should be emphasized here that the latter two results were obtained by totally different numerical techniques (Jordinson used the finite-difference technique and Benek used the Chebyshev polynomial approximation technique), and thus the modes of the P and S families which were found cannot be attributed to numerical inaccuracies because in both of these investigations the authors reported finding eigenmodes that belong to these families as well as some that belong to the A family.

In attempting to determine numerically the spectrum for the semi-infinite problem, all that can be done is to solve successively a number of finite interval problems over the range $[0, y_1]$, increasing y_1 gradually to larger values, and hope to arrive at an asymptotic form of the spectrum as $y_1 \rightarrow \infty$. Such an attempt was undertaken in this study and, as far as the numerical calculations allowed, we always found an infinite discrete spectrum no matter how large y_1 was taken. However, as y_1 became large, the number of eigenvalues of the P and S families grew larger and their separation became smaller. Also, with the increase of the value of y_1, the lines along which these families lie shifted towards the line $c_r = 1$. This investigation was not able to verify whether or not a limit at $c_r = 1$ exists for these families. However, as Figure 11 shows, a limit might exist for some value of $c_r \leqslant 1$.

It may be concluded from these observations that as the interval of numerical integration $[0, y_1]$ goes to $[0, \infty)$, the eigenvalue spectrum for the boundary layer flow profile may be composed of two parts: one continuous which is comprised of a straight line at $c_r = 1$, and the other discrete and finite comprised of the members of the A family. However, for practical purposes in which the problem is solved numerically over a finite range of integration, the spectrum will then be considered to be infinite and discrete. The only way to resolve this question will be through a rigorous mathematical proof.

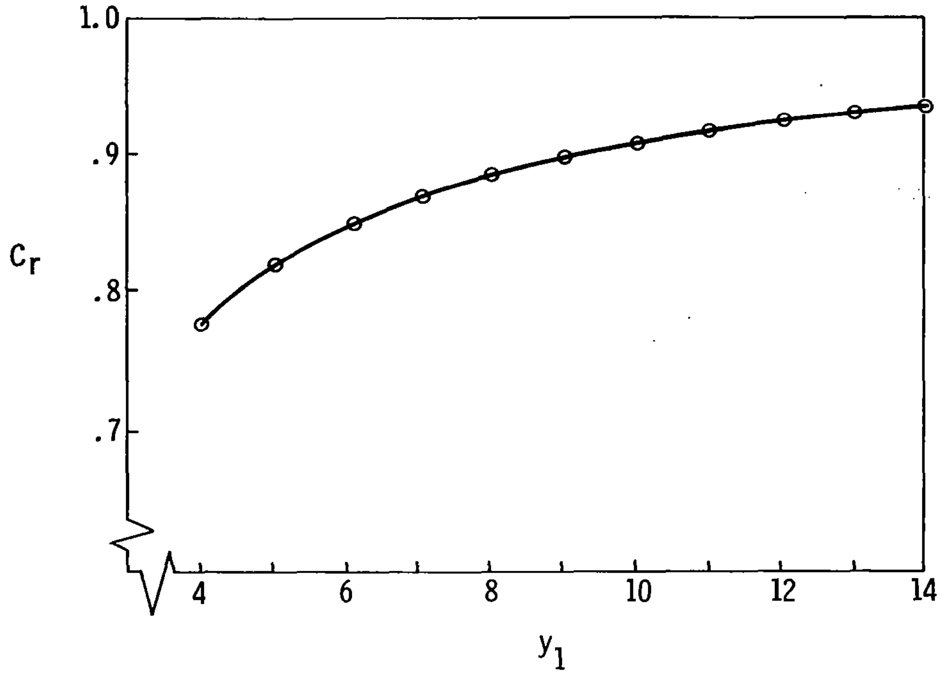

Figure 11. Variation of the value of c_r with y_1 for a typical member of the S family for the Blasius boundary layer flow at α = 0.308 and R = 998.

This investigation may be concluded with some remarks on the utility of the numerical search technique used here. A global numerical technique has been outlined for use in solving linear differential eigenvalue problems. The technique is general and automatic, requiring a minimum of information from the operator. The technique is also deterministic and does not require any a priori knowledge on the location of the eigenvalues. Furthermore, if high accuracy on the eigenvalues is not desired, the present method is sufficient for the solution of the eigenvalue problem. However, when high accuracy is required, the present scheme may be used to search for the eigenvalues and, once located, their approximate location may be input into a local method that will converge fast enough to the desired accuracy on the eigenvalues and the eigenfunctions. Thus, this method could save considerable time by eliminating the trial and error procedure and the guesswork that might be involved when using a local technique.

REFERENCES

1. Lin, C.C.: The Theory of Hydrodynamic Stability. Cambridge University Press, Cambridge, 1966.

2. McHugh, James A. M.: An Historical Survey of Ordinary Linear Differential Equations with a Large Parameter and Turning Points. Arch. Hist. Exact Sci., vol. 7, 1971, p. 277.

3. Eckhaus, Wiktor: Studies in Non-Linear Stability Theory. Springer-Verlag, Berlin and Heidelberg, 1965.

4. Schensted, Irene V.: Contributions to the Theory of Hydrodynamic Stability. Ph.D. dissertation, University of Michigan, 1960.

5. DiPrima, R.C. and Habetler, G.J.: A Completeness Theorem for Non-Selfadjoint Eigenvalue Problems in Hydrodynamic Stability. Arch. Rat. Mech. and Anal., vol. 34, 1969, p. 218.

6. Jordinson, R.: Spectrum of Eigenvalues of the Orr-Sommerfeld Equation for Blasius Flow. Phys. Fluids, vol. 14, 1971, p. 2535.

7. Mack, L.M.: A Numerical Study of the Temporal Eigenvalue Spectrum of the Blasius Boundary Layer. J. Fluid Mech., vol. 73, 1976, p. 497.

8. Jordinson, R.: The Flat Plate Boundary Layer. Part I, Numerical Integration of the Orr-Sommerfeld Equation. J. Fluid Mech., vol. 43, 1970, p. 801.

9. Benek, John A.: The Effects of Periodic Free Stream Disturbances on the Flat Plate Boundary Layer. Ph.D. dissertation, University of Tennessee, 1975.

10. Mack, L.M.: Computation of the Stability of the Laminar Compressible Boundary Layer. Methods of Comp. Physics, vol. 4, B. Alder, ed., Academic Press, New York, 1965.

11. Davey, A.: A Simple Numerical Method for Solving Orr-Sommerfeld Problems. Q. J. Mech. and Appl. Math., vol. 26, 1973, p. 401.

12. Lee, L.H. and Reynolds, W.C.: On the Approximate and Numerical Solution of Orr-Sommerfeld Problems. Q. J. Mech. and Appl. Math., vol. 20, 1967, p. 1.

13. Naimark, M.A.: Linear Differential Operators, Part I. Frederick Ungar, New York, 1967.

14. Goodstein, R.L.: Complex Functions. McGraw-Hill, New York, 1965.

15. Delves, L.M. and Lyness, J.N.: A numerical Method for Locating the Zeros of an Analytic Function. Math. Comp., vol. 21, 1967, p. 543.

16. Fehlberg, Erwin: Classical Eighth- and Lower-Order Runge-Kutta-Nyström Formulas with Stepsize Control for Special Second-Order Differential Equations. NASA TR R-381, 1972.

17. Godunov, S.: On the Numerical Solution of Boundary Value Problems for Systems of Linear Ordinary Differential Equations. Uspehi Mat. Nauk., vol. 16, 1961, p. 171.

18. Conte, S.D.: The Numerical Solution of Linear Boundary Value Problems. S.I.A.M. Rev., vol. 8, 1966, p. 309.

19. Antar, Basil N.: On the Solution of Two-Point Linear Differential Eigenvalue Problems. J. Comp. Phys., vol. 20, 1976, p. 209.

NASA-Langley, 1976